Journal of Marine Science and Technology

Volume 31 | Issue 2 | Article 3

Multi-chamber Silencer Composed of Screw-perforated Tubes and Straight-perforated Tubes

Tian-Syung Lan
School of Intelligent Engineering, Shaoguan University, Guangdong, 512005, China, tslan@ydu.edu.tw

Min-Chie Chiu
Department of Mechanical and Materials Engineering, Tatung University, Taiwan, ROC, mcchiu@gm.ttu.edu.tw

Recommended Citation
Lan, Tian-Syung and Chiu, Min-Chie (2023) "Multi-chamber Silencer Composed of Screw-perforated Tubes and Straight-perforated Tubes," *Journal of Marine Science and Technology*: Vol. 31: Iss. 2, Article 3.
DOI: 10.51400/2709-6998.2687
Available at: https://jmstt.ntou.edu.tw/journal/vol31/iss2/3

RESEARCH ARTICLE

Multi-chamber Silencer Composed of Screw-perforated Tubes and Straight-perforated Tubes

Tian-Syung Lan [a,b], Min-Chie Chiu [c,*]

[a] School of Intelligent Engineering, Shaoguan University, Guangdong, 512005, China
[b] Department of Information Management, Yu Da University of Science and Technology, Miaoli County, 361, Taiwan, ROC
[c] Department of Mechanical and Materials Engineering, Tatung University, Taiwan, ROC

Abstract

The use of silencers to reduce noise is mandatory due to severe hearing damage caused by high venting noise in the engine room of ocean-going vessels. While straight and perforated tubes have been used as acoustical elements in traditional silencer design, studies have shown that the acoustical design still requires improvement. To enhance acoustical efficiency, the use of multi-chamber mufflers is proposed composed of screw and perforated tubes. Additionally, a mathematical finite element model built for acoustical simulation using the COMSOL program expedites the analysis of silencers with complicated acoustical elements. A sensitivity analysis of transmission loss concerning the geometric factors of two-chamber and three-chamber silencers is conducted to investigate the relationship between sound transmission loss and silencer shape. The results demonstrate that the multi-chamber silencer with screw tubes and straight perforated tubes performs well in reducing noise.

Keywords: FEM, Multiple chamber, Screw, Perforated

1. Introduction

The use of acoustical tubes as an element embedded in silencers is widespread. Perforated tubes, straight and bent, have been employed to mitigate venting noise. Rostafinski [1] analyzed sound attenuation in a bent duct through an acoustic model. Fuller and Bies [2,3] investigated the impact of acoustical performance with regards to ducts of varying section area and shape. Kim and Ih [4] estimated sound transmission loss of a bent and expansion chamber using a four-pole transfer matrix method. Yeh et al. [5] discussed the acoustical effect of a linearly expanded tube. Chiu and Chang [6] studied optimally shaped cross-flow tubes embedded in a multiple chamber silencer. Chiu [7] evaluated the acoustical elimination ability of reverse-flow ducts installed inside a one-chamber silencer. Additionally, Chiu [8] explored multiple parallel perforated plug tubes implanted inside a two-chamber silencer.

Noise issues are significant in factories on land [9] and on ships at sea. Due to the loud noises emitted by marine diesel engines on boats [10], the use of silencers to reduce venting noise from engines and protect hearing is mandatory [11]. However, as mentioned previously, the studies discussed were limited to low-frequency regions using plane wave theory. To address the acoustical effect in higher frequency domains, Fang et al. [12] analyzed the pressure loss of a muffler using a CFD model. Chiu developed a system composed of multiple connected tubes using the boundary element method [13], while Chen and Shi evaluated exhaust muffler efficiency using CFD [14]. Moreover, there has been significant progress in the development and

Received 16 January 2023; revised 23 February 2023; accepted 30 March 2023.
Available online 30 June 2023

* Corresponding author at: Department of Mechanical and Materials Engineering, Tatung University, No.40, Sec.3, Zhongshan N. Rd., Taipei, 10452, Taiwan, ROC.
E-mail address: mcchiu@gm.ttu.edu.tw (M.-C. Chiu).

https://doi.org/10.51400/2709-6998.2687

utilization of sound-absorbing materials for noise reduction purposes. For instance, Chang et al. [15] developed a mathematical model for a single-layer sound absorber, while Chiu [16] presented a mathematical model of a single-chamber silencer internally lined with sound-absorbing wool.

A novel acoustical device with multiple chambers, screw/perforated tubes, and internal lining with sound-absorbing wool has been developed to enhance the sound elimination capabilities. The device includes four types of silencers: Silencer A, a two-chamber silencer with a straight-perforated tube; Silencer B, a two-chamber silencer with a screw-perforated tube; Silencer C, a three-chamber silencer with a straight-perforated tube; and Silencer D, a three-chamber silencer with two screw-perforated tubes and a straight-perforated tube. Due to the complexity of the silencers' structures, the Finite Element Method (FEM) has been consistently used to analyze the acoustical field. As such FEM simulations were run on COMSOL to enable acoustical analysis of the complicated-shaped silencers (Silencer A to Silencer D).

2. Mathematical calculation of the FEM (on COMSOL)

As shown in Figs. 1 and 2, four types of silencers have been developed, consisting of multiple cavities with screw/perforated tubes, straight/perforated tubes, and internally lined with wool. A solid boundary was used in the COMSOL model as the boundary condition for the acoustical field.

$$n\bullet\left\{\frac{1}{\rho_c}(\nabla p_t-q)\right\}=0 \tag{1}$$

where $p_t = p + p_b$, p is acoustic pressure, and p_b is the background noise. q is a dipole sound source, c is sound speed, and ρ is air density.

The boundary condition of the perforated tube (a solid boundary) in sound field is

$$n\bullet\left\{\frac{1}{\rho_c}(\nabla p_t-q)\right\}=-(p_{t1}-p_{t2})\frac{i\omega}{Z_i} \tag{2}$$

$$Z_i=\rho_c c_c\left[\left[\frac{1}{\sigma}\right]\sqrt{\frac{8\mu k}{\rho_c c_c}}\left(1+\frac{t_p}{d_h}\right)+\theta_f+i\frac{k}{\sigma}(t_p+\delta_h)\right] \tag{3}$$

The Johnson-Champoux-Allard model was used to simulate the acoustical field of porous material, as follows:

$$\rho_{eff}=\alpha_\infty\rho_0\left(1+\frac{\sigma_0\varphi}{j\rho_0\omega\alpha_\infty}G_J(\omega)\right) \tag{4}$$

Nomenclature	
C	sound speed and set as 343 (m/s)
d_h	the hole's diameter of the perforated tube (m)
K_{eff}	bulk factor
pt1, pt2	the upstream acoustic pressure and downstream acoustic pressure (Pa)
R	acoustical flow impedance of sound absorbing wool ($kg/m^3.s$)
q	a dipole sound source and set at zero
TL	transmission loss (dB)
t_p	the thickness of the perforated tube (m)
Z_i	acoustic impedance ($Pa\cdot s/m^3$)
σ	perforation ratio for the screw perforated tube and straight/perforated tube (%)
ρ	air density and set at 1.293 (kg/m^3)
α_∞	curvature level
η	shearing viscosity($=1.84\times10^{-5}kg/ms$)
φ	porosity of sound absorbing material
σ	perforation rate of a perforated tube
σ_0	acoustical flowing impedance
χ	viscous character length
χ'	thermal character length

$$G_J(\omega)=\left(1+\frac{4j\alpha_\infty^2\eta\rho_0\omega}{\alpha_0^2\chi^2\varphi^2}\right)^{1/2} \tag{5}$$

where η is the shearing viscosity, φ is the wool porosity, α_∞ is the curvature, and σ_0 is the impedance expressed as

$$\sigma_0=\frac{\mu}{\alpha}=\frac{150\mu(1-\varphi)^2}{D_p^2\varphi^3} \tag{6}$$

In addition, K_{eff} (the bulk factor) is

$$K_{eff}=\frac{\gamma P_0}{\gamma-(\gamma-1)\left[1+\frac{8\eta}{j\wedge^2B^2\omega\rho_0}\left(1+j\rho_0\frac{\omega B^2\wedge^2}{16\eta}\right)^{\frac{1}{2}}\right]^{-1}} \tag{7}$$

Both χ (viscous character length) and χ' (thermal character length) yield

$$\chi=\frac{1}{c}\left(\frac{8\alpha_\infty\eta}{\sigma_0\varphi}\right)^{1/2} \tag{8}$$

$$\chi'=\frac{1}{c'}\left(\frac{8\alpha_\infty\eta}{\sigma_0\varphi}\right)^{1/2} \tag{9}$$

The derivation equation of sound wave propagation is

$$-\nabla\cdot\frac{1}{\rho_c}(\nabla(p+p_b)-q)-\frac{k_{eq}^2(p+p_b)}{\rho_c} \tag{10a}$$

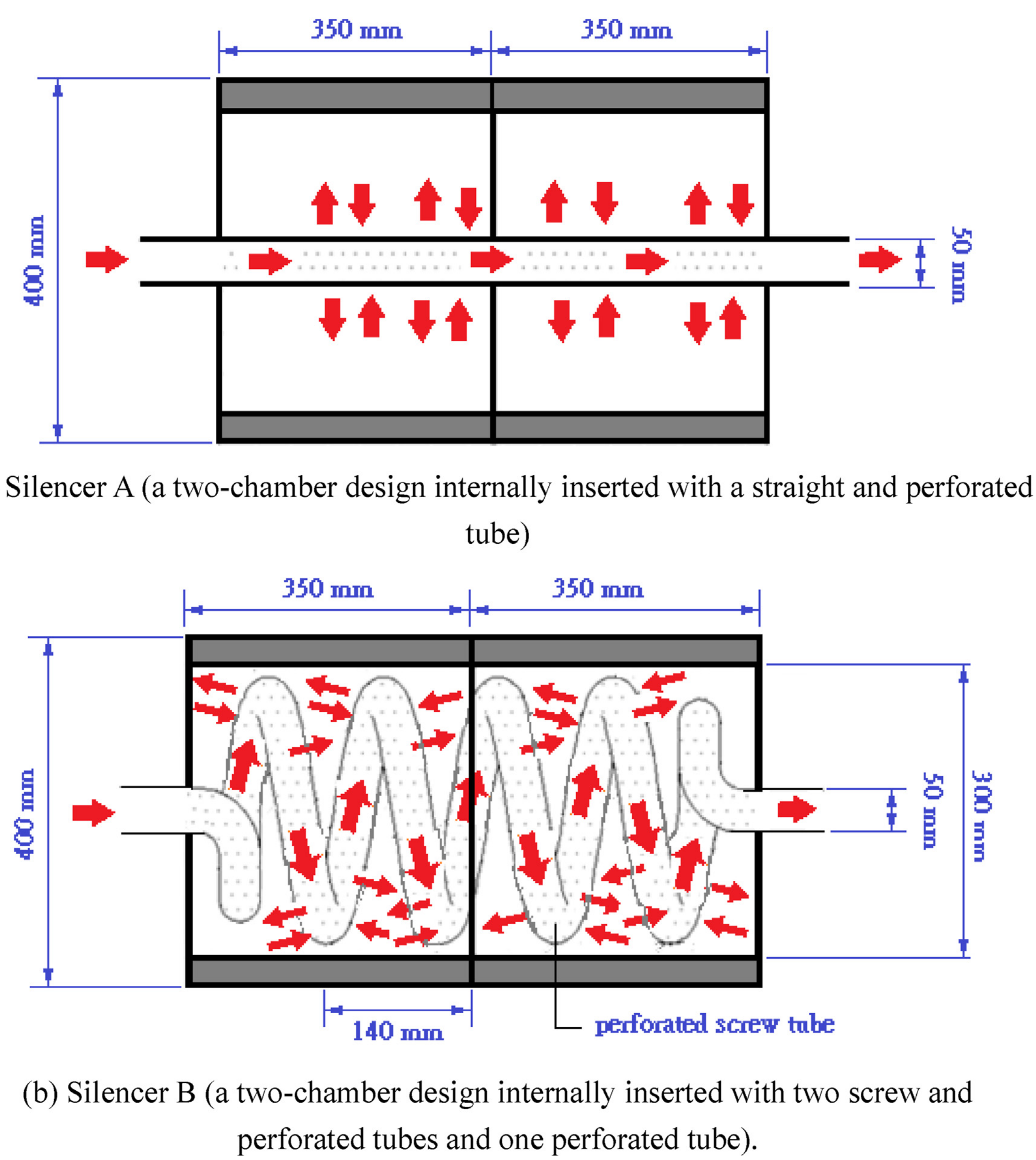

Fig. 1. Acoustical mechanisms of silencer A and silencer B.

where

$$k_{eq}^2 = \left(\frac{\omega}{c_c}\right)^2;\ c_c = c;\ \rho_c = \rho \tag{10b}$$

The Transmission Loss (TL) of silencer is

$$\mathrm{TL} = 10\log\frac{W_{in}}{W_{out}} \tag{11}$$

3. Model check

An experiment was conducted using a silencer with a straight perforated tube to validate the accuracy of the FEM model, as shown in Fig. 3. The TL profile of this silencer was compared with experimental data provided by Jeon et al. [17]. The comparison showed that the TL profiles were similar, with the maximum errors occurring at the peak ranging from 2 to 5 dB. The accuracy of the COMSOL using FEM was deemed acceptable and, therefore, used in the subsequent analysis. The FEM model built in this study was considered reliable.

4. Results and discussion

4.1. Results

Four types of silencers were developed with different combinations of acoustical elements.

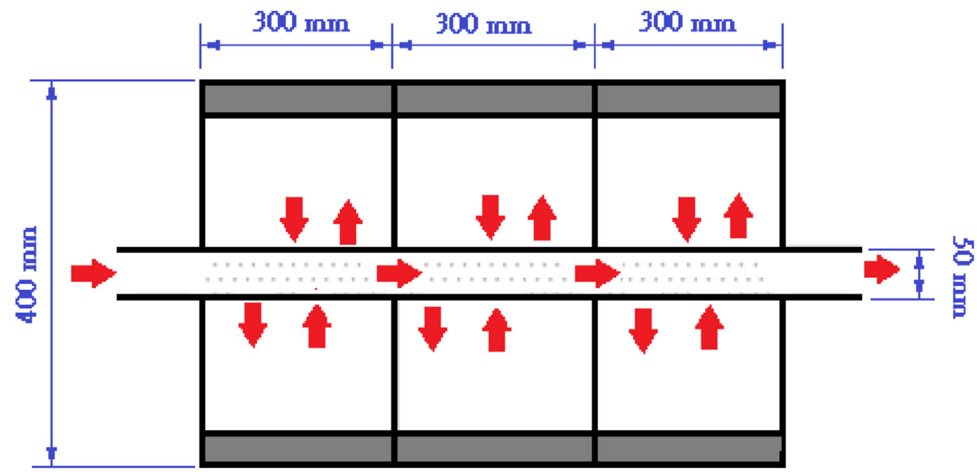

(a) Silencer C (a three-chamber design internally inserted with a straight and perforated tube silencer)

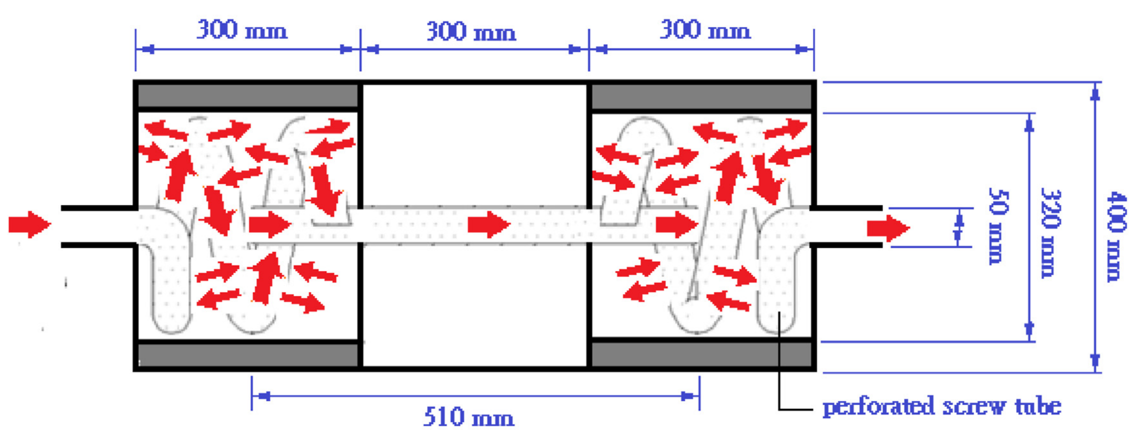

(b) Silencer D (a three-chamber design internally inserted with two screw/ perforated tubes and one perforated tube).

Fig. 2. Acoustical mechanisms of silencers C and D.

Silencer A is a two-chamber silencer with a straight-perforated tube, while Silencer B is a two-chamber silencer with a screw-perforated tube. Silencer C is a three-chamber silencer with a straight-perforated tube, and Silencer D is a three-chamber silencer with two screw-perforated tubes and a straight-perforated tube. The Transmission Loss (TL) of Silencers A and B was compared in Fig. 4, and the TL of Silencer B was found to be higher than that of Silencer A. Therefore, Silencer B, a two-chamber muffler with a screw-perforated tube, was chosen for further acoustical sensitivity analysis. In the analysis process, the acoustical flow resistance of the wool (R), shown in Fig. 5, was selected as the design parameter. The simulated results in Fig. 6 indicated that an increase in R has a positive effect on the increment of TL. The perforation ratio of the screw and perforated tube (σ) shown in Fig. 7 was also selected, and the predicted TL was found to increase when the perforation ratio decreased, as shown in Fig. 8.

Silencers C and D were further examined after analyzing silencers A and B, as shown in Fig. 2. Silencer C is a three-chamber muffler with a straight-perforated tube, while silencer D is a three-chamber muffler with two screw-perforated tubes and one straight-perforated tube. The simulated TL profiles for silencers C and D are compared in Fig. 9,

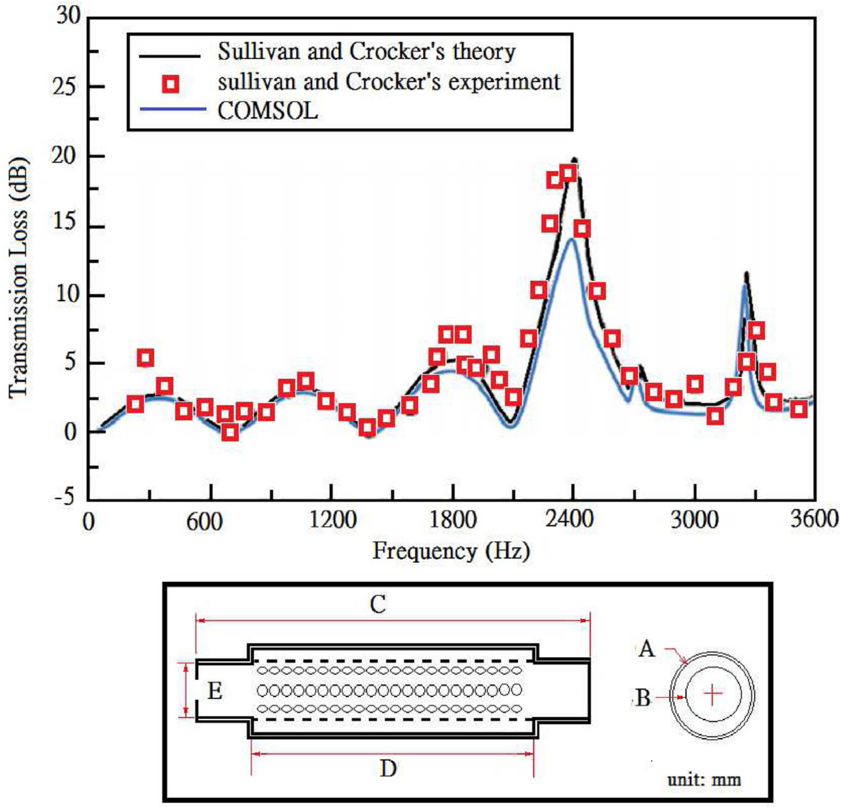

Fig. 3. Accuracy check of sound transmission loss for silencers internally inserted with a straight and perforated tube (A = 76.2, B = 52.42, C = 357.2, D = 257.2, E = 50.8) [17].

indicating that silencer D performs significantly better than silencer C. Therefore, silencer D is chosen for sensitivity analysis of the perforation ratio (σ), as shown in Fig. 10. The simulation results in Fig. 11 demonstrate that as the perforation ratio decreases, the estimated TL increases.

4.2. Discussion

Silencer B exhibits better noise reduction ability compared to silencer A thanks to the bent shape effect, as discussed in section 4.1 and shown in Fig. 4. The predicted results in Figs. 6 and 8

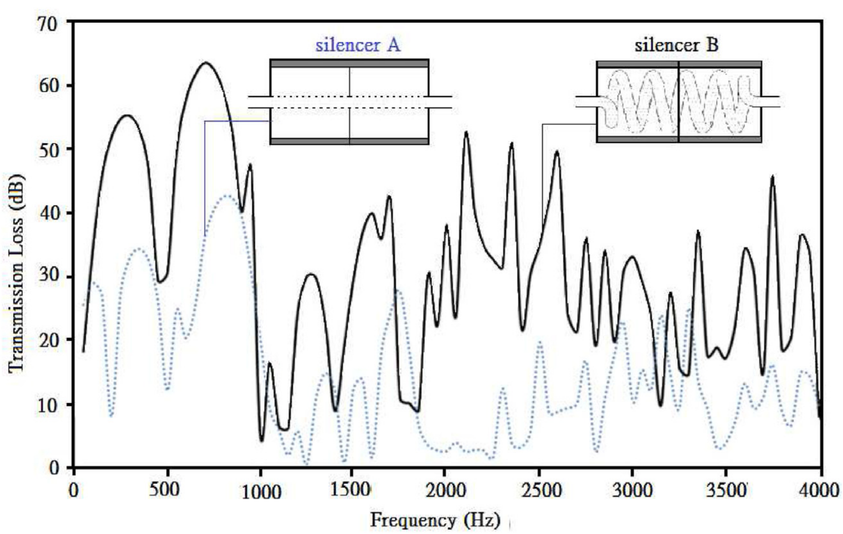

Fig. 4. A comparison of TL between silencer A and silencer B.

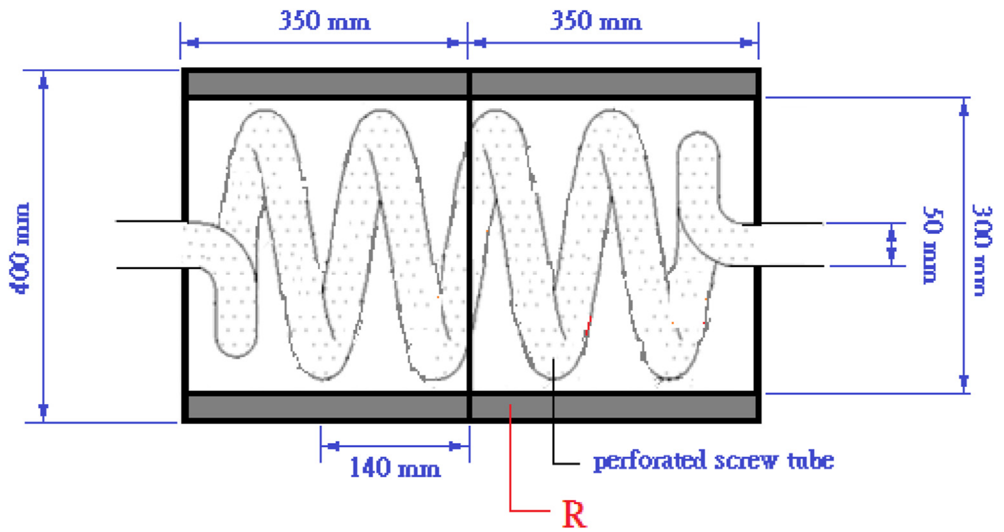

Fig. 5. A selected parameter of R (acoustical flow resistance of wool internally lined inside the silencer B).

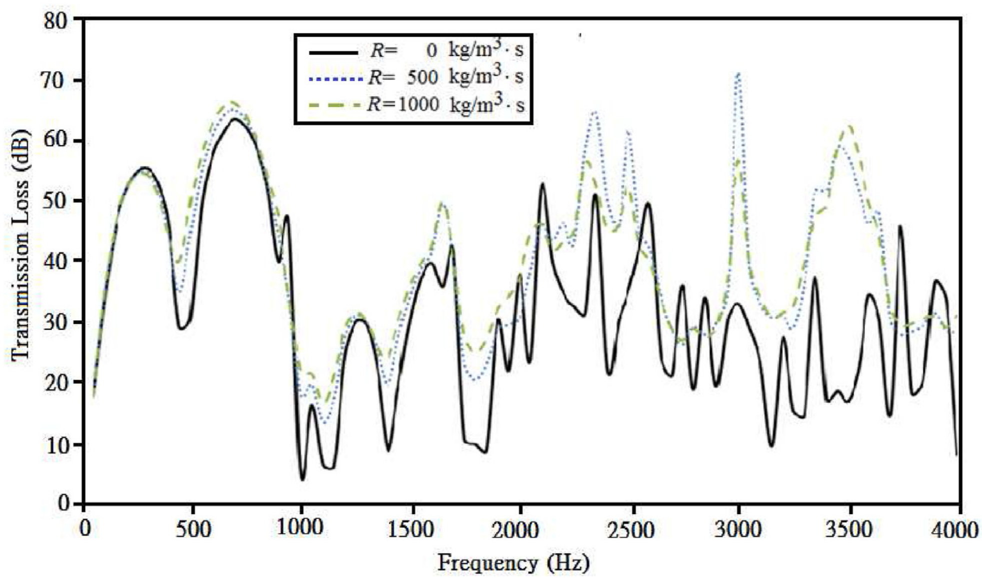

Fig. 6. The acoustical influence of TL with respect to R (the acoustical flow resistance) in silencer B (σ = 5%).

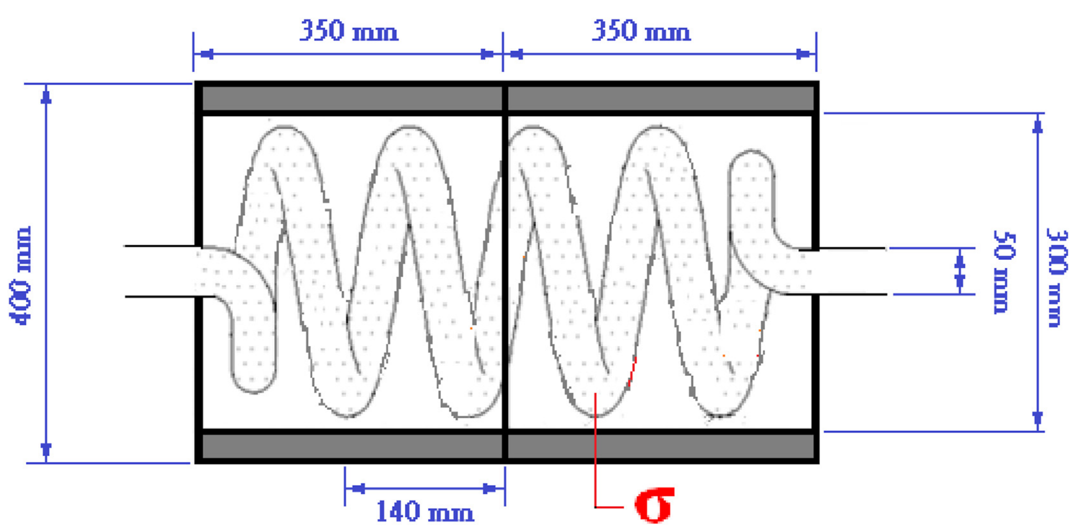

Fig. 7. A selected parameter of σ (perforation ratio of the screw and perforated tube for silencer B).

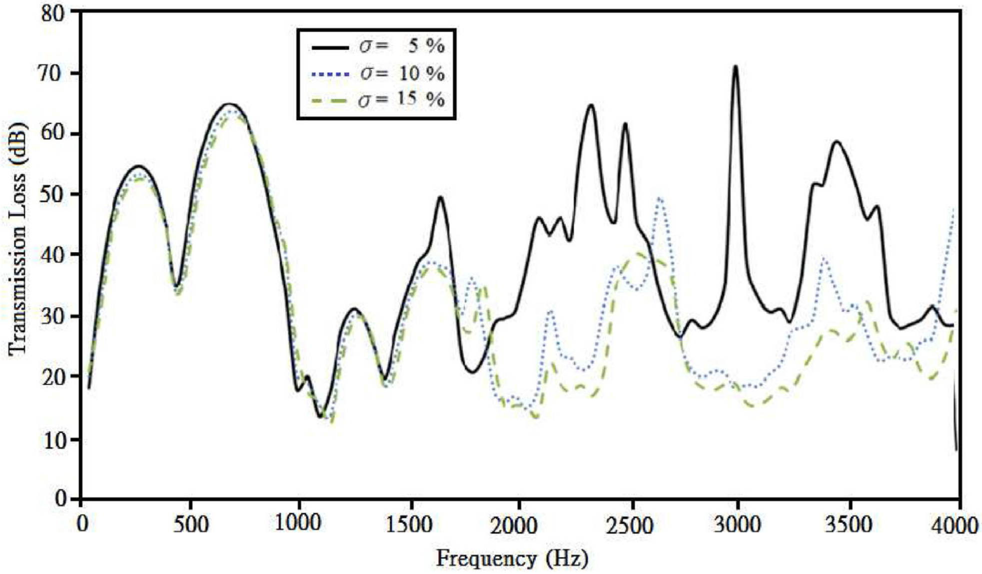

Fig. 8. The acoustical influence of TL with respect to σ (perforation ratio of the screw and perforated tube) in silencer B (R = 500 kg/m^3).

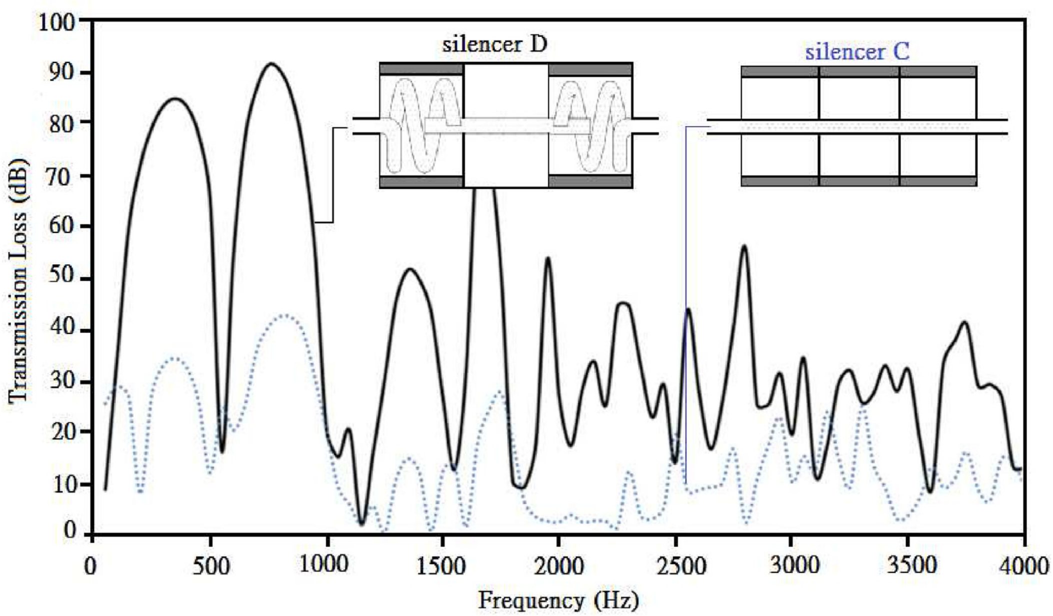

Fig. 9. A comparison of TL between silencer C and silencer D.

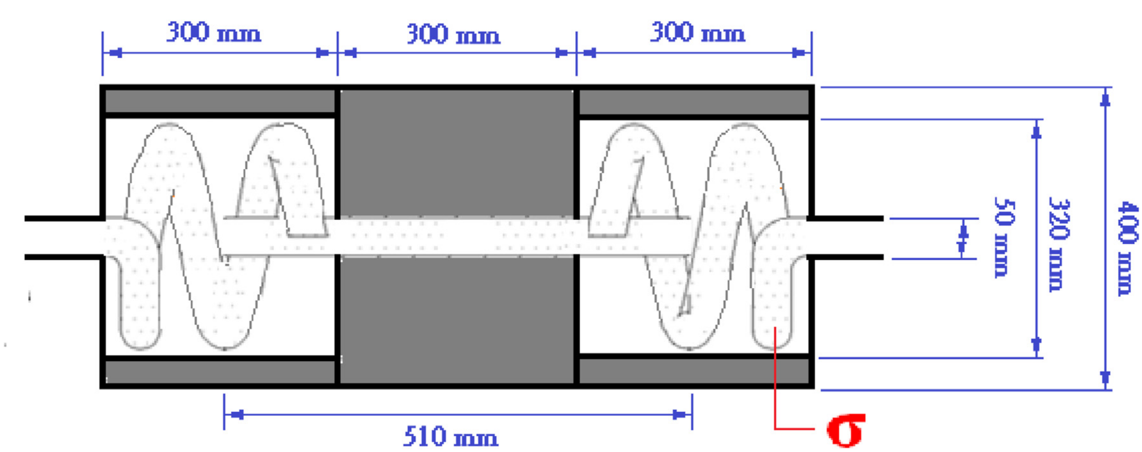

Fig. 10. A selected parameter of σ (perforation ratio of the screw and perforated tube for silencer D).

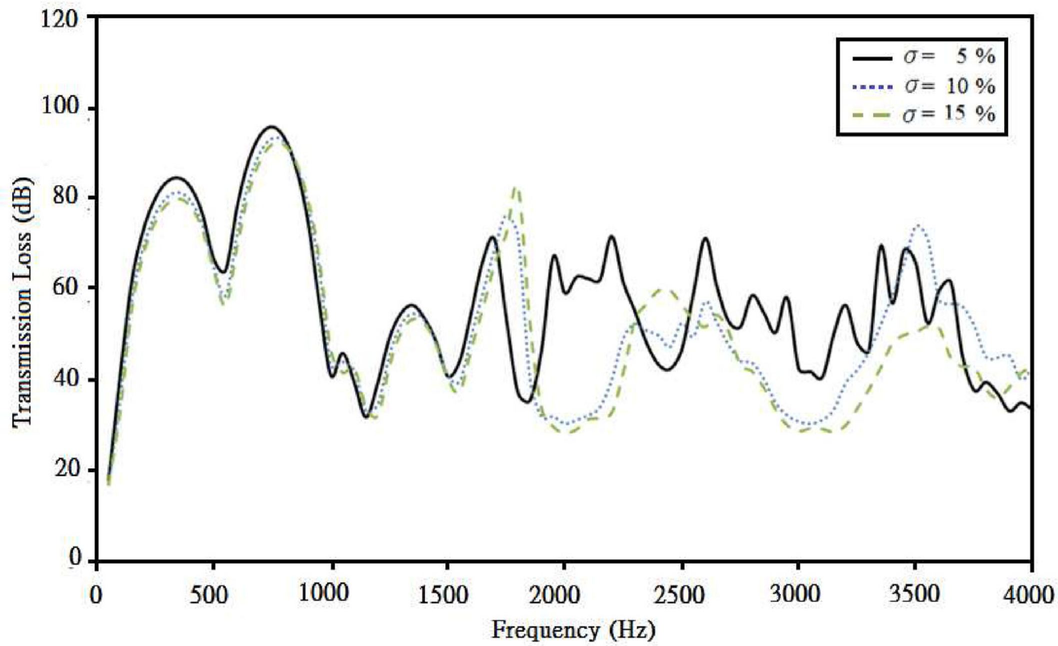

Fig. 11. Acoustical influence of TL with respect to σ (perforation ratio of the screw and perforated tube) in silencer D (R = 500 kg/m³).

demonstrate that both R (acoustical flow resistance of wool) and σ (perforation ratio of the screw and perforated tube) have a significant impact on TL. The TL increases with R increases, and decreases with σ. Furthermore, as seen in Fig. 9, the TL of silencer D is far greater than that of silencer C, which could be attributed to the curved shape effect. Assuming of the same R for all silencers, the simulation results presented in Fig. 11 suggest that σ also has a significant impact on TL, with the noise reduction ability increasing as σ decreases.

A comparison of TL for all silencers was performed by inserting the screw tube into both the two-chamber silencer (silencer B) and the three-chamber silencer (silencer D), as shown in Fig. 12. It is observed that silencer D has better TL than silencer B when the frequency is below 2000 Hz. However, the acoustical effect fluctuates between

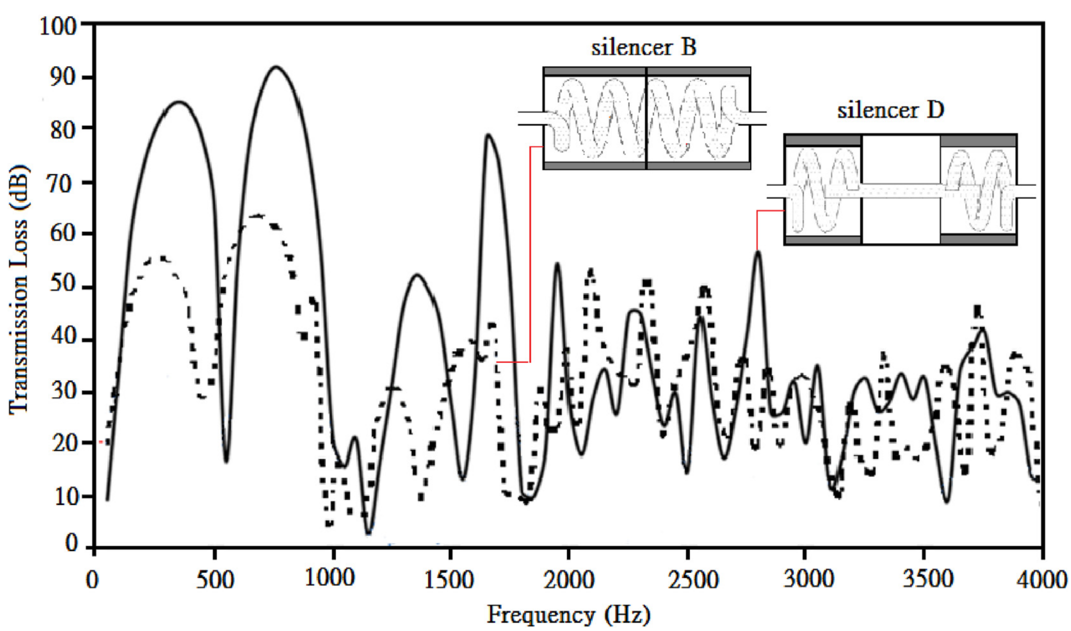

Fig. 12. A comparison of TL between silencer B and silencer D (at σ = 5% and R = 0 kg/m₃.s).

the two-chamber silencer B and three-chamber silencer D when the frequency is higher than 2000 Hz, indicating that the number of chambers has a noticeable impact in the lower frequency region.

5. Conclusion

Four types of silencers (silencers A-D) were analyzed acoustically for the purpose of the study, and the results showed that silencer B performed better than silencer A in noise reduction thanks to the screw tube effect. The impact of silencer B's geometric factors on TL was also examined, revealing that both the perforation ratio (σ) and the acoustical flow resistance of wool (R) played important roles in the acoustical performance. TL was found to be directly proportional to R and inversely proportional to σ. A comparison of silencer C and silencer D demonstrated that the curved shape of the tube inserted in the silencer results in higher TL. Additionally, with the same R value for silencer D, TL increased when σ decreased. As discussed in section 4.2, silencer D has a better acoustical effect at lower frequencies (below 2000 Hz) because it has a larger number of chambers. Therefore, this paper provides a design guideline for silencer designers on how to choose appropriate acoustical elements and geometric design parameters for multi-chamber silencers implanted with curved (screw) and straight perforated tubes.

Conflict of interest

The authors declare that there are no conflicts of interest regarding the publication of this paper.

References

[1] Rostafinski W. Transmission of wave energy in curved ducts. J Acoust Soc Am 1974;56:1005–7.
[2] Fuller CR, Bies DA. A reactive acoustic attenuator. J Sound Vib 1978;56(1):45–59.
[3] Fuller CR, Bies DA. Propagation of sound in a curved bend containing curved axial partition. J Acoust Soc Am 1978;63: 681–6.
[4] Kim JT, Ih JG. Transfer matrix of curved duct bends and sound attenuation in curved expansion chambers. Appl Acoust 1999;56:297–309.
[5] Yeh LJ, Chang YC, Chiu MC. Shape optimization on constrained linearly expanded tubes by using genetic algorithm. Tech Acoust 2003;18:1–11.
[6] Chiu MC, Chang YC. Shape optimization of multi-chamber cross-flow Mufflers by SA optimization. J Sound Vib 2008; 312:526–50.
[7] Chiu MC. Shape optimization of one-chamber mufflers with reverse-flow ducts using a genetic algorithm. J Mar Sci Technol 2010;18(1):12–23.
[8] Chiu MC. Numerical assessment of two-chamber mufflers hybridized with multiple parallel perforated plug tubes using simulated annealing method. J Low Freq Noise Vib Act Control 2017;36(1):3–26.
[9] Yeh LJ, Chang YC, Chiu MC. Numerical studies on constrained venting system with reactive mufflers by GA optimization. Int J Numer Methods Eng 2006;65:1165–85.
[10] Bogdanowicz A, Kniaziewicz T. Marine diesel engine exhaust emissions measured in ship's dynamic operating conditions. Sensors 2020;20(6589):1–21.
[11] Lee TK, Joo WH, Bae JG. Exhaust noise control of marine diesel engine using hybrid silencer. Transac Korean Soc Noise Vibr Eng 2009;19(7):679–84.
[12] Fang J, Zhou Y, Jiao P, Ling Z. Study on pressure loss for a muffler based on CFD and experiment, 2009 international conference on measuring technology and mechatronics automation. 2009.
[13] Chang YC, Chiu MC, Wu LW. Shape optimization of mufflers hybridized with multiple connected tubes using boundary element method and neural networks and genetic algorithm. Proc ImechE Part C: J Mech Eng Sci 2010;224(C4):901–13.
[14] Chen J, Shi X. CFD numerical simulation of exhaust muffler. In: 2011 Seventh international conference on computational intelligence and security; 2011.
[15] Chang YC, Yeh LJ, Chiu MC, Lai GJ. Shape optimization on constrained single-layer sound absorber by using GA method and mathematical gradient methods. J Sound Vib 2005;286(4–5):941–61.
[16] Chiu MC. Shape optimization of one-chamber perforated mufflers filled with wool using simulated annealing. J Mar Sci Technol 2013;21(4):380–90.
[17] Jeon S, Kim D, Hong C, Jeong W. Acoustic performance of industrial mufflers with CAE modeling and simulation. Int J Nav Archit Ocean Eng 2014;6(4):935–46.